Journal of ELECTRONIC MATERIALS, Vol. 43, No. 6, 2014
DOI: 10.1007/s11664-014-2992-x

Thermoelectric Properties of Al-Doped ZnO Thin Films

S. SAINI,[1,6] P. MELE[1,7], H. HONDA[2] K. MATSUMOTO,[3] K. MIYAZAKI,[4] and A. ICHINOSE[5]

1.—Institute for Sustainable Sciences and Development, Hiroshima University, Higashi-Hiroshima 739-8530, Japan. 2.—Graduate School for Advanced Sciences of Matter, Hiroshima University, Higashi-Hiroshima 739-8530, Japan. 3.—Department of Material Science, Kyushu Institute of Technology, Kitakyushu 804-8550, Japan. 4.—Department of Mechanical Engineering, Kyushu Institute of Technology, Kitakyushu 804-8550, Japan. 5.—Electric Power Engineering Research Laboratory, CRIEPI, Yokosuka 240-0196, Japan. 6.—e-mail: ssaini@hiroshima-u.ac.jp. 7.—e-mail: pmele@hiroshima-.ac.jp

We have prepared 2 % Al-doped ZnO (AZO) thin films on $SrTiO_3$ substrates by a pulsed laser deposition technique at various deposition temperatures (T_{dep} = 300–600 °C). The thermoelectric properties of AZO thin films were studied in a low temperature range (300–600 K). Thin film deposited at 300 °C is fully *c*-axis-oriented and presents electrical conductivity 310 S/cm with Seebeck coefficient −65 μV/K and power factor 0.13 × 10^{-3} Wm^{-1} K^{-2} at 300 K. The performance of thin films increases with temperature. For instance, the power factor is enhanced up to 0.55 × 10^{-3} Wm^{-1} K^{-2} at 600 K, surpassing the best AZO film previously reported in the literature.

Key words: Thermoelectric, ZnO thin films, PLD, Seebeck, power factor

INTRODUCTION

The need for energy production and conservation in the industralized world has generated interest in effective alternative energy approaches, to overcome the dependence of mankind on traditional energy sources (carbon, oil, and fossil fuel) and to reduce CO_2 emissions. Thermoelectric materials are considered extremely interesting from the sustainable point of view because they can convert thermal energy to electrical energy.[1] The efficiency of thermoelectric energy conversion is determined by the dimensionless figure of merit $ZT = (\sigma \times S^2) \times T/\kappa$ (where S is the Seebeck coefficient, σ is the electrical conductivity, κ is the thermal conductivity, and T is the absolute temperature).[2] Because of their poor conversion efficiency (below 20 % for Bi_2Te_3-based devices),[3] thermoelectric materials have been restricted for a long time to a scientific scope.[4] Efforts have been made worldwide to enhance the performance of thermoelectric materials[5] (i.e. the value of ZT) by increasing values of S and σ and at the same time lowering the value of κ as much as possible.

In the past few decades, materials such as silicon-germanium alloys,[6] metal chalcogenides,[7] boron compounds,[8] and many more have been developed for thermoelectric applications. The performance of these materials have been remarkable. For example, the value of ZT for metallic thermoelectric Bi_2Te_3/Sb_2Te_3 multi-layered films was reported to be up to 2.5 at T = 300 K.[9] However, their practical applications have been limited because of low temperature decomposition, oxidation, vaporization, or phase transition. These limitations have stimulated a lot of research on oxides as thermo-electric materials, because they are thermally and electrically stable in air at high temperatures.

Among oxides, ZnO has always been attracted much attention because of its versatile applications such as optical devices in the ultraviolet region,[10] piezoelectric transducers,[11] transparent electrodes for solar cells,[12] gas sensors,[13,14] and many more.[15,16] A ZnO *n*-type semiconductor is a potentially low-cost, nontoxic, stable thermoelectric material that can be used up to very high temperatures because its decomposition temperature is more than 2,000 °C. Pure and doped bulk ZnO has been studied as

S. Saini and P. Mele contributed equally to this study.
(Received June 26, 2013; accepted January 2, 2014; published online January 23, 2014)

thermoelectric materials for space applications, solar-thermal and electrical-energy production, and so on.[17,18]

Thin film materials are advantageous over bulk because of their light weight, quick response time, and compact size for modules or sensors. For example, enhancement of thermoelectric power in Si-Ge-Au amorphous thin films[19] and Bi_2Te_3/Sb_2Te_3 super lattice thin films[20] have been previously reported. However, there are very few works on thermoelectric ZnO thin films,[21,22] in which the highest reported value of the power factor is 1.79×10^{-4} W/mK^2 at 643 K.[21] Thermoelectric ZnO thin films have not been sufficiently explored, even if they are relatively easy to prepare.[23,24] The main reason is the practical difficulty in the measurement of thermoelectric properties at high temperature. In this work, we have investigated 2 % Al-doped ZnO thin films (AZO) fabricated by pulsed laser deposition (PLD). We will discuss the structural, electrical, and thermal properties of AZO thin films deposited at different temperatures on $SrTiO_3$ (STO) single crystals.

EXPERIMENTAL DETAILS

The AZO thin films were grown by the PLD technique using a Nd:YAG laser (266 nm, 10 Hz). A pellet of $Zn_{0.98}Al_{0.02}O$ (20 mm in diameter and 3 mm in thickness) prepared by spark plasma sintering was used as the target to grow the thin films. The 2 % Al was chosen as the best doping in bulk.[25] A detailed description of sintered target growth is reported elsewhere.[26] The laser was fired onto the dense AZO target with a energy density of about 4.2 J/cm^2 for a deposition period of 30 min. Thin films were deposited on $SrTiO_3$ 100 (STO) substrates at 300, 400, 500, and 600 °C under an oxygen pressure of 200 mTorr. AZO thin films on STO show lower lattice mismatch $\epsilon_{c,STO} = -2\,\%$ than on $Al_2O_3 \epsilon_{c,Al_2O_3} = 18\,\%$. Lattice mismatch ($\epsilon_c$) can be calculated as for STO; $\epsilon_{c,STO} = \frac{\sqrt{3}a_{AZO} - 2a_{STO}}{2a_{STO}}$ and for Al_2O_3; $\epsilon_{c,Al_2O_3} = \frac{\sqrt{3}a_{AZO} - a_{c,Al_2O_3}}{a_{c,Al_2O_3}}$, where a_{AZO}, a_{STO}, and $a_{Al\_2O\_3}$ are a-axis lengths for AZO, STO, and Al_2O_3, respectively. The target was rotated during the irradiation of the laser beam. The STO substrates were glued with silver paste on an inconel plate customized for ultrahigh vacuum applications. The thickness of the thin films were kept about 500 nm. Deposition parameters, such as laser pulse frequency 10 Hz, substrate–target distance about 35 mm, and rotation speed of the target 30 % rpm, were kept unchanged during all the deposition routes.

The structural characterization was done by x-ray diffraction (XRD) (Bruker D8 Discover, USA) and morphology was checked by scanning electron microscope (SEM) (JEOL, FESEM, Japan). The thickness and in-plane roughness were obtained by 3D-microscope Keyence VK-9700 (Keyence, Japan). The electrical conductivity versus temperature (σ–T) characteristics were measured by a conventional four-probe technique from 300 to 600 K with a hand-made apparatus consisting of a current source (ADCMT 6144, ADCMT Japan), temperature controller (Cryo-con 32, USA), and nano-voltmeter (Keithley 2182A, USA). The Seebeck coefficient was measured by a commercially available system (MMR Technologies, USA) in the temperature range 300–600 K. Carrier concentrations at room temperature were evaluated by means of a Quantum Design PPMS (Quantum Design, USA).

RESULTS AND DISCUSSION

The effect of deposition temperature on AZO thin films surface was investigated using SEM and is shown in Fig. 1. Thin films deposited at 300 and 500 °C are highly connected and dense, presenting round-shaped grains with diameters in the range 20–150 nm. The film deposited at 600 °C has a completely different morphology, with smaller and elongated grains (length ≈50–100 nm and size about 10 nm) with many pores and is less connected. The 400 °C deposited samples is further different: compact (no pores appear) with wider distribution of grain sizes. It is very difficult to find a simple correlation between deposition temperature and evolution of grain size and morphology.

Figure 2 shows XRD patterns of the films which have only peaks belonging to a wurtzite hexagonal structure. Secondary phases such as $ZnAl_2O_4$ did not form during the thin film deposition process. Films deposited at 300 and 400 °C show only a (002) peak indicating fully c-axis orientation of AZO on STO. An additional (110) peak, corresponding to a-axis orientation, appears on increasing the deposition temperature to 500 and 600 °C. Indeed, the sample deposited at 600 °C also presents the (100) peak. The modulation of c-axis/a-axis orientations of pure and doped ZnO thin films by single crystal substrate engineering has been extensively reported in the literature.[27–33] According to the intensity of the (002) peak, the sample deposited at 300 and 400 °C have the best crystallinity. The lattice mismatch of AZO on STO can be calculated as −2 and −6 % for c-axis and a-axis orientation, respectively. Despite such relatively large values, there is no effect on the crystalline parameters of the films, which remain almost unchanged with respect to the bulk values (Table I).

The dependence of grain size and lattice parameter (c-axis and a-axis length) on deposition temperature is summarized in Fig. 3. Furthermore, AZO films deposited on STO at 400 and 600 °C show several pores, while the films fabricated at 300 and 500 °C are well connected.

Transport and thermoelectric properties of thin films are summarized in Table I. Figure 4a shows electrical conductivity versus temperature (σ–T) for AZO thin films. σ increases with temperature, with

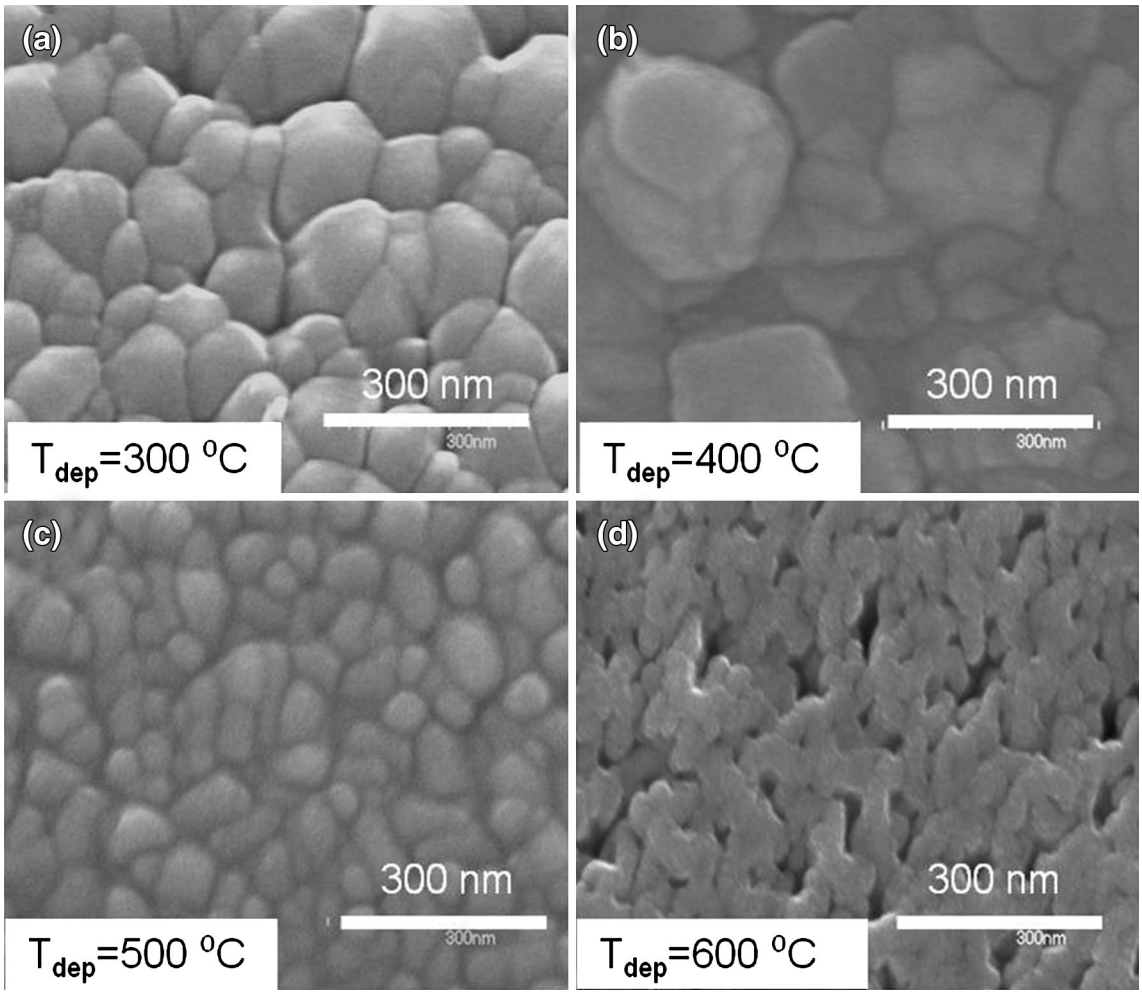

Fig. 1. SEM image of AZO thin films deposited at different temperature (T_{dep} = (a) 300 °C, (b) 400 °C, (c) 500 °C, and (d) 600 °C).

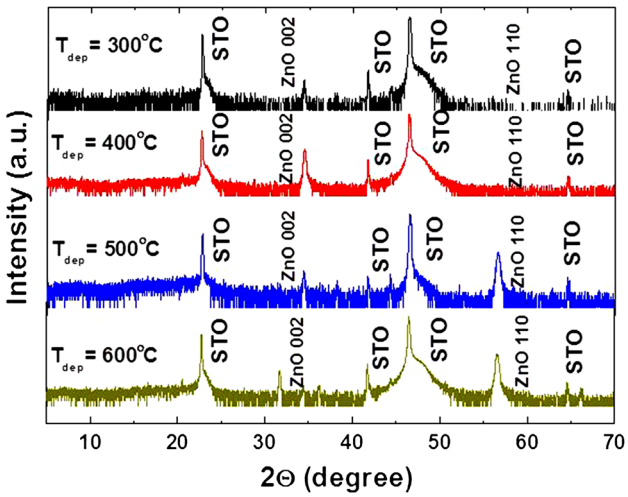

Fig. 2. 2θ-XRD pattern of AZO thin films deposited at different temperature (T_{dep} = 300, 400, 500, and 600 °C).

a typical semiconducting behavior. The increasing deposition temperature leads to a decrease of electrical conductivity. Focusing on room temperature data, the film deposited at 300 °C shows the highest electrical conductivity (about 310 S/cm) while the film deposited at 600 °C shows electrical conductivity of 32 S/cm at room temperature, lower than the bulk material (206 S/cm).[26]* The trend of electrical conductivity cannot be simply related to the microstructure of the films, otherwise the samples deposited at 300 and 500 °C, which present similar amounts and sizes of grains, should have similar values of σ. Indeed, as reported in Table I, there is no direct proportionality between carrier concentration and electrical conductivity: for example, the sample with the highest carrier concentration (T_{dep} = 400 °C) is the second sample in terms of σ. Furthermore, the carrier concentrations of our films are far from the value 10^{20} cm^{-3}, reported as optimal for thermoelectric properties;[34] this is probably due to the oxygen atmosphere used in the deposition.

*For bulk AZO, the value of S, σ, and power factor at 300 K are taken by extrapolation of S and σ from Mele et al.[26]

Table I. Electrical and thermal parameters for thin films and bulk pellet of AZO at 300K/600K

Sample	*a*-axis (Å)	*c*-axis (Å)	Electrical conductivity (σ) (S/cm)	Carrier concentration (n) (10^{19} cm^{-3})	Seebeck coefficient (S) (μV/K)	Power factor (PF) (10^{-3} W/m K^2)
T_{dep} = 300 °C	–	5.21	310/382	0.12	−65/−121	0.13/0.55
T_{dep} = 400 °C	–	5.20	98/133	2.55	−90/−163	0.08/0.32
T_{dep} = 500 °C	3.25	5.21	71/77	0.02	−151/−245	0.15/0.43
T_{dep} = 600 °C	3.25	5.21	32/45	0.03	−138/−214	0.06/0.19
Bulk AZO[26] and see Footnote 1	3.25	5.20	206/152	–	−132/−150	0.35/0.34

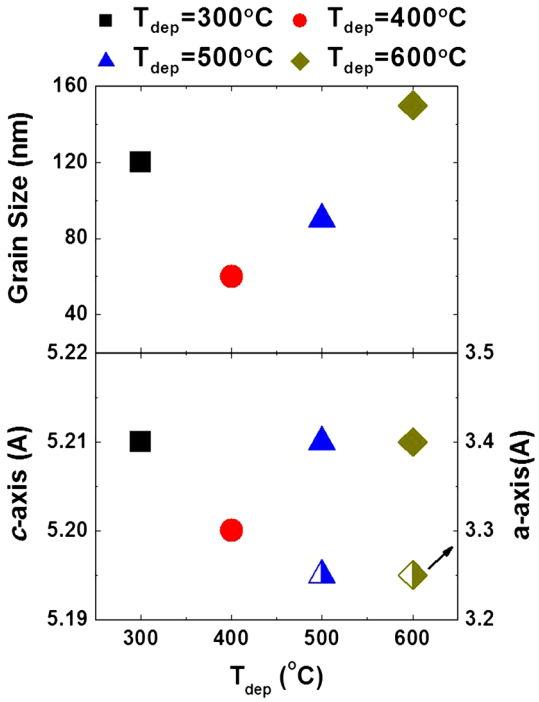

Fig. 3. Influence of deposition temperature on morphology and structural properties of AZO thin films: grain size and *a*-axis (half-filled symbol) and *c*-axis length (filled symbol).

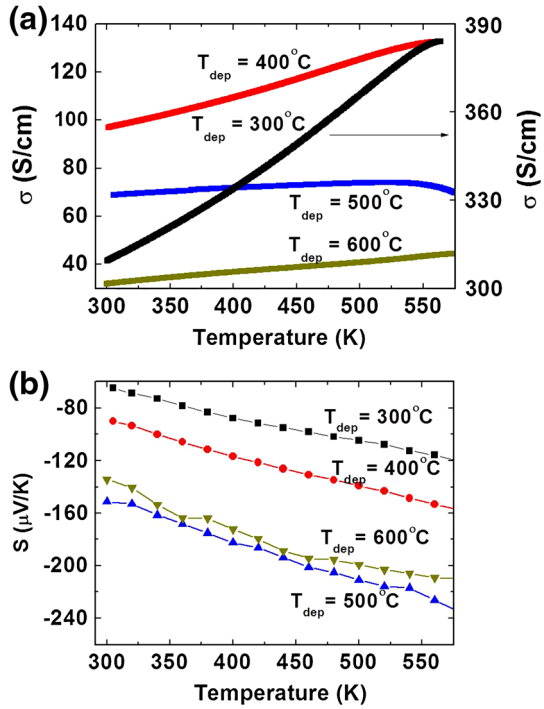

Fig. 4. (a) Electrical conductivity vs temperature (σ–T) characteristics, (b) Seebeck coefficient versus temperature (S–T) characteristics of thin films for various deposition temperatures (300–600 °C) at different operating temperatures (300 K and 600 K).

Overall, to explain the electrical conductivity behavior of the films, it is possible to invoke the anisotropy of σ with the crystallographic orientation: fully *c*-axis-oriented samples (deposited at 300 and 400 °C) possess the highest electrical conductivity, followed by the sample with *c*- and *a*-axis orientation (500 °C), and eventually by the polycrystalline sample deposited at 600 °C. This is quite similar to the scenario reported by Abutaha et al.[35] for AZO films deposited on $LaAlO_3$ single crystals at T = 573–1,273 °C. The main difference with our AZO-STO samples is their extremely large size (941 S/cm at 300 K for best *c*-axis-oriented film) and the presence of fully *a*-axis-oriented films. At the maximum T available (600 K), our films maintain the same trend, decreasing with deposition temperature: the best value is 382 S/cm for the sample deposited at 300 °C, while the sample deposited at 600 °C has only 45 S/cm.

The plots of Seebeck coefficient versus temperature (S–T) are reported in Fig. 4b. The trend of S with the deposition temperature is opposite with respect to σ except for the sample deposited at 500 °C that has the largest values of S: −151 and −245 μV/K at 300 and 600 K, respectively. In general, we obtained larger values of S than Abutaha et al.[35] (−33 μV/S in their best case). Typical values reported in the same range of temperature for thin films and bulk materials (−150 μV/K at 673 K,[17] −110 μV/K at 650 K[36]) were also surpassed.

From the values of the Seebeck coefficient and electrical conductivity, we have calculated the power factor (PF) of thin films as PF = $\sigma \times S^2$ (Fig. 5a). At 300 K, the sample deposited at 500 °C has the largest power factor, 0.15 × 10^{-3} W/mK^2, due to the fact that S is very large (see Table I). However, with increasing temperature, the PF of

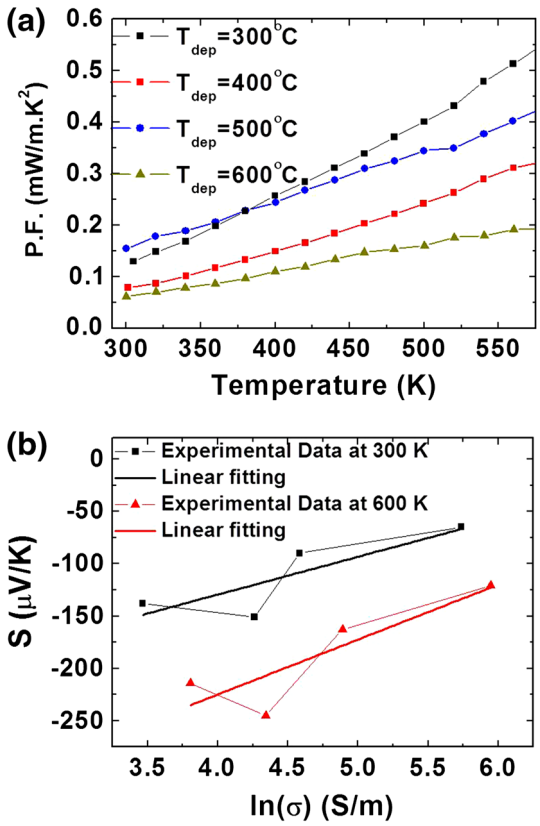

Fig. 5. (a) Power factor vsersu temperature plot, (b) Jonker plot (Seebeck coefficient vs natural logarithm of conductivity) of thin films for various deposition temperatures (300–600 °C) at different operating temperatures (300 and 600 K).

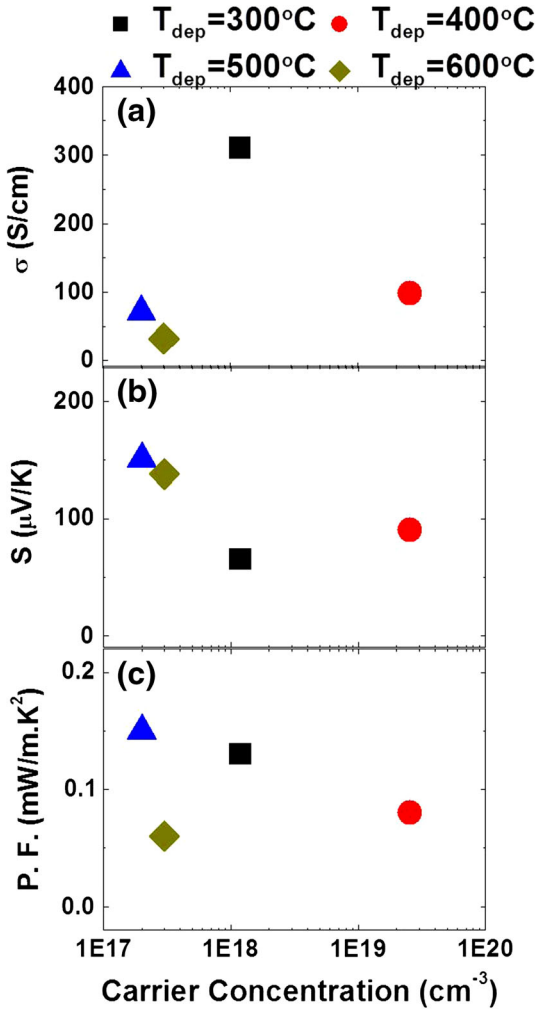

Fig. 6. Room temperature values of (a) electrical conductivity, (b) Seebeck coefficient and (c) power factor in terms of logarithmic carrier concentration for AZO thin films deposited at 300, 400, 500, and 600 °C.

the sample deposited at 300 °C becomes the largest and eventually is 0.55×10^{-3} W/mK^2 at 600 K. The value of PF has enhanced in comparison with previous reports for AZO thin films (maximum value reported so far being 0.35×10^{-3} W/mK^2 at 740 K,[35] while a typical value for bulk sample is reported up to 1.5×10^{-3} W/mK^2 at 1,000 °C.[37]

The correlation of the power factor with carrier concentration requires further investigations to be clarified. For n-type semiconductors like AZO, at a constant temperature the value of σ and S is expressed as follows:

$$\left.\begin{aligned} \sigma &= n.e.\mu \\ S &= -\frac{k_B}{e}\left(\ln\frac{N_c}{n} + A\right) \end{aligned}\right\}, \quad (1)$$

where n is the carrier concentration, μ is the mobility, k_B is the Boltzmann constant, N_c is the density of states, and A is a transport constant.[38] The optimum condition to achieve the highest power factor can be written from the above equation as

$$\left.\begin{aligned} n_{optimum} &= N_c \exp(A-2) \\ \sigma_{optimum} &= e\mu N_c \exp(A-2) \end{aligned}\right\}. \quad (2)$$

The value of $e\mu N_c \exp(A-2)$ can be estimated from the Jonker plot[39] which establishes a relationship between the Seebeck coefficient and conductivity, i.e.

$$S = \frac{k}{e}[\ln\sigma - \ln e\mu N_c \exp(A)], \quad (3)$$

where k/e is the slope and $\ln e\mu N_c \exp(A)$ is the intersection with the x-axis of the plot of the Seebeck coefficient and the natural logarithm of conductivity. The Jonker plot of thin films for various deposition temperatures (300–600 °C) at different operating temperatures (300 and 600 K) is shown in Fig. 5b. The value of the slope of the data is 36 μV/K for 300 K and 53 μV/K for 600 K which is lower than k/e (86.15 μV/K). The maximum value of the power factor can be predicted by Ioffe analysis[34] by the intersection $(\ln e\mu N_c \exp(A))$ derived from the Jonker

plot. The maximum value of the power factor from the intersection is 0.1 μW/m K^2 for 300 K and 0.6 μW/m K^2 for 600 K.

The strong deviation of our experimental results from the Jonker plot and Ioffe analysis may be ascribed to the non-linearity of mobility with carrier concentration. It is reasonable to argue that the nature of substrate, as well as the doping level, film thickness, oxygen pressure, and deposition temperature, play a crucial role in the mobility/concentration interplay. These aspects will be investigated in our future work.

Trends of σ, S and PF with carrier concentration at room temperature are reported in Fig. 6. At 300 K, the sample deposited at 500 °C has the largest power factor, 0.15×10^{-3} W/mK^2, due to the fact that S is very large. However, with increasing temperature, the PF of the sample deposited at 300 °C becomes the largest and eventually is 0.55×10^{-3} W/mK^2 at 600 K. The value of PF has enhanced in comparison with previous reports for AZO thin films (maximum value reported so far being 0.35×10^{-3} W/mK^2 at 740 K,[35] while a typical value for bulk sample is reported up to 1.5×10^{-3} W/mK^2 at 1,000 °C.[37]

SUMMARY

In summary, the thermoelectric material $Zn_{0.98}Al_{0.02}O$ (AZO) was grown as thin films by the PLD technique at various deposition temperatures (T_{dep} = 300, 400, 500, and 600 °C) on STO substrates. The value of the electrical conductivity of thin films deposited at 300 °C was 310 S/cm at 300 K, higher than for thin films deposited at 400, 500, and 600. The absolute value of S for AZO thin films was in the range of 90–245 μV/K and the value of the power factor (PF) was in range of $0.06 \sim 0.55 \times 10^{-3}$ W/m K^2. For the whole temperature range (300–600 K), we have observed that the film deposited at 300 °C shows the highest value of the power factor. Overall, the best performance was observed in fully c-axis-oriented thin films deposited at 300 °C with $S = -121$ μV/K, and PF = 0.55×10^{-3} W/m K^2 at 600 K. This represents the optimum data so far for AZO films deposited on single crystals. We expect further improvements in thermoelectric performance by carrying on the deposition in reduced atmosphere to increase the carrier concentration of the film, which is far from the optimal value expected for thermoelectric materials (10^{20} cm^{-3}). The nature of the substrate, the doping level, and film thickness may represent other crucial parameters that will be investigated in our future work.

REFERENCES

1. T.J. Seebeck, *Abh. Akad. Wiss. Berlin* 289, 1820 (1822).
2. H. Böttner, *Mater. Res. Soc. Symp. Proc.* N01-01, 1166 (2009).
3. D.M. Rowe, *Thermoelectrics Handbook: Macro to Nano* (Boca Raton: CRC/Taylor & Francis, 2006).
4. A. Majumdar, *Science* 303, 777 (2004).
5. T.M. Tritt and M.A. Subramanian, *MRS Bull.* 31, 188 (2006).
6. N.F. Hinsche, I. Mertig, and P. Zahn, *J. Phys. Condens. Matter* 24, 275501 (2012).
7. D. Baoli, Y. Saiga, K. Kajisa, and T. Takabatake, *J. Appl. Phys.* 111, 013707 (2012).
8. C. Wood and D. Emin, *Phys. Rev. B* 29, 4582 (1984).
9. R. Venkatasubramanian, E. Siivola, T. Colpitts, and B. O'Quinn, *Nature* 413, 517 (2001).
10. G.M. Ali and P. Chakrabarti, *J. Phys. D Appl. Phys.* 43, 415103 (2010).
11. P.X. Gao and Z.L. Wanga, *J. Appl. Phys.* 97, 044304 (2005).
12. M. Law, L.E. Greene, J.C. Johnson, R. Saykally, and P. Yang, *Nat. Mater.* 4, 455 (2005).
13. M. Kaur, S.V.S. Chauhan, S. Sinha, M. Bharti, R. Mohan, S.K. Gupta, and J.V. Yakhmi, *J. Nanosci. Nanotechnol.* 9, 5293 (2009).
14. R. Mohan, K. Krishnamoorthy, and S.-J. Kim, *Solid State Commun.* 152, 375 (2012).
15. R. Mohan and S.-J. Kim, *Jpn. J. Appl. Phys.* 50, 04DJ01 (2011).
16. Z.L. Wang, *Mater. Sci. Eng. R* 64, 33 (2009).
17. M. Ohtaki, T. Tsubota, K. Eguchi, and H. Arai, *J. Appl. Phys.* 79, 1816 (1996).
18. J.P. Wiff, Y. Kinemuchi, and K. Watari, *Mater. Lett.* 63, 2470 (2009).
19. H. Uchino, Y. Okamoto, T. Kawahara, and J. Morimoto, *Jpn. J. Appl. Phys.* 39, 1675 (2000).
20. R. Venkatasubramanian, E. Siivola, T. Colpitts, and B. O'Quinn, *Nature* 413, 597 (2001).
21. Y. Inoue, M. Okamoto, T. Kawahara, Y. Okamoto, and J. Morimoto, *Mater. Trans.* 46, 1470 (2005).
22. K.P. Ong, D.J. Singh, and P. Wu, *Phys. Rev. B* 83, 115110 (2011).
23. J. Mass, P. Bhattacharya, and R.S. Katiyar, *Mater. Sci. Eng.* B103, 9 (2003).
24. B. Singh, Z.A. Khan, I. Khan, and S. Ghosh, *Appl. Phys. Lett.* 97, 241903 (2010).
25. P. Mele, K. Matsumoto, T. Azuma, K. Kamesawa, S. Tanaka, J. Kurosaki, and K. Miyazaki, *Mater. Res. Soc. Symp. Proc.* 1166, 3 (2009).
26. P. Mele, H. Kamei, H. Yasumune, K. Matsumoto, and K. Miyazaki, *Met. Mater. Int.* (2013). doi:10.1007/s12540-014-2024-7.
27. G. Sun, K. Zhao, Y. Wu, Y. Wang, N. Liu, and L. Zhang, *J. Phys. Condens. Matter* 24, 295801 (2012).
28. Y.-T. Ho, W.-L. Wang, C.-Y. Peng, M.-H. Liang, J.-S. Tian, C.-W. Lin, and L. Chang, *Appl. Phys. Lett.* 93, 121 (2008).
29. M. Snure and A. Tiwari, *J. Appl. Phys.* 101, 124912 (2007).
30. D.H. Cho, J.H. Kim, B.M. Moon, Y.D. Jo, and S.M. Koo, *Appl. Surf. Sci.* 235, 3480 (2009).
31. L.C. Nistor, C. Ghica, D. Matei, G. Dinescu, M. Dinescu, and G. Van Tendeloo, *J. Cryst. Growth* 277, 26 (2005).
32. J.S. Tian, M.H. Liang, Y.T. Ho, Y.A. Liu, and L. Chang, *J. Cryst. Growth* 310, 777 (2008).
33. H.P. Sun, X.Q. Pan, X.L. Du, Z.X. Mei, Z.Q. Zheng, and Q.K. Xue, *Appl. Phys. Lett.* 85, 4385 (2004).
34. A. Loffe, *Semiconductor Thermoelements and Thermoelectric Cooling* (London: Infosearch Ltd., 1957).
35. A.I. Abutaha, S.R. Sarath Kumar, and H.N. Alshareef, *Appl. Phys. Lett.* 102, 053507 (2013).
36. H. Hiramatsu, H. Ohta, W.-S. Seo, and K. Koumoto, *J. Jpn. Soc. Powder Powder Metall.* 44, 44 (1997).
37. T. Tsubota, M. Ohtaki, K. Eguchi, and H. Arai, *J. Mater. Chem.* 7, 85 (1996).
38. Q. Zhu, E.M. Hopper, B.J. Ingram, T.O. Mason, *J. Am. Ceram. Soc.* 94, 187 (2011).
39. G. Jonker, *Philips Res. Report* 23, 131 (1968).